NUMERICAL ANALYSIS OF MICRO-STRUCTURED MATERIALS EFFECT ON ELECTROMAGNETIC FIELD SHIELDING IN A WIDE FREQUENCY RANGE

Laura IONEL[1], Aurelian MARCU[1]

The interaction of high-intensity light sources with solid targets generates intense broadband electromagnetic (EM) pulses in a wide frequency range, from radio frequency to x-rays with multiple biological effects at cellular level. In this work, we elaborated a 3D numerical model to investigate the behavior of particular shielding materials and to compare their performances at some different frequencies, considered as relevant both for the generated frequencies and for the cell's absorbed wavelengths under the conditions imposed by high energy experiments planned to be performed at facilities in ultra-intense regime. The 3D numerical simulations of the electromagnetic field shielding have been made using Finite-Difference Time-Domain (FDTD) method to design and investigate different structures both as metallic foil or mesh and to evaluate their efficiency in a wide frequency regime (100 – 4000 MHz) being relevant for EM shielding in various light–matter interaction experiments in ultra-intense regime.

Keywords: electromagnetic field, finite-difference time-domain, shielding cage, microstructure, high-intensity light sources.

1. Introduction

The recent progresses made in the development of high-intensity light sources open new perspectives of fundamental physics and also impact applications from laboratory astrophysics and inertial confinement fusion to laser matter interaction in ultra-intense regimes. The interaction of ultra-intense light sources with solid targets produces intense broadband electromagnetic pulses in a large frequency regime, from radio frequency to x-rays. In the petawatt regime, these intense electromagnetic radiations are expected to be emitted in the GHz to THz domain, being also called Giant Electro-Magnetic Pulses (GEMP) [1-4]. Nowadays, there are a multitude of shielding materials with properties able to provide specific levels of radioprotection. For a high level of protection, beside the optimum mechanical properties of the shielding materials, the external factors such as humidity, damages caused by the high dose of radiation or extreme temperatures should be also took into account before the shielding project to be designed [5,6]. Moreover, the nuclear reactions produced by the laser – solid target interactions may activate the

[1] Researcher, National Institute for Laser, Plasma and Radiation Physics, Romania, e-mail: laura.ionel@inflpr.ro, aurelian.marcu@inflpr.ro

shielding materials to behave as radiation secondary sources [7,9]. All these aspects beside other particular issues [10-13] should be carefully managed for a correct risk evaluation before each high-power laser experiment [14,15].

In order to provide a complex estimation of the biological effects of the electromagnetic waves over the living cells on particular wavelengths during further high-intensity light sources – matter interaction experiments and considering the GEMP spectra generated during real experiments, we had performed 3D numerical simulations to investigate the behavior of particular shielding materials having different profiles by using a scaled configuration setup. The main objective is to compare the performances of this material at some different frequencies, considered as relevant both for the generated frequencies and for the human cell's absorbed wavelengths under the conditions imposed by high energy experiments. The electromagnetic field shielding study is performed for particular experimental configurations numerically simulated using Finite-Difference Time-Domain (FDTD) method using FullWave and CAD packages of the commercial software RSoft (by Synopsys Optical Solution Group) [16]. Lately, a plenty of FDTD studies had been elaborated in order to determine the optimum conditions for extreme electric field generation [17-23]. A detailed study concerning the electromagnetic field shielding under high-intensity light irradiation conditions has been elaborated using different structures both as metallic foil or mesh in order to measure its efficiency in a wide frequency regime (100-4000 MHz).

2. Numerical approach

Starting from the cell's response on particular wavelengths, a 3D numerical model had been elaborated in order to investigate the behavior of particular shielding materials at different frequencies under the conditions imposed by light–matter interaction experiments planned to be performed at facilities in ultra-intense regime. The 3D numerical simulations have been developed using FULLWAVE and CAD packages of the commercial software RSoft. Reasonable assumptions on the irradiation conditions were made, given the fact that these aspects will be different in each experiment.

In order to determine an appropriate level of radioprotection during the interaction of high-intensity light source with different targets, an advanced study of different shielding materials has been performed. For this, the 3D numerical simulations have been done by taking into consideration the specifications in terms light source parameters and irradiation chamber technical details. With the respect to the real size of the irradiation chamber (13.5x12x5.5 m) and its wall thickness (1.5-2 m) a scaled 3D configuration of a classical bunker has been designed in order to investigate the efficiency of several preconfigured shielding structures positioned in the vicinity of the irradiation point.

In the frame of the electromagnetic field parameters investigation in frequency domain, the numerical analysis is expressed as a Fourier Sum which is calculated using a discretized Fourier Transform evaluated over a finite domain:

$$\bar{\Phi}(r',\omega) = \sum_{t=0}^{t_s} \Phi(r',t) e^{i\omega t} dt \tag{1}$$

where $\varphi(r',t)$ represents the data recorded by the time monitors, ω is the frequency and t_s is the simulation stop time.

For a more detailed study, the electromagnetic field shielding behavior has been investigated in a wide frequency range (100 – 4000 MHz) in order to evaluate with high precision, the material shielding efficiency, in predefined conditions.

3. Numerical results and discussions

The 3D numerical simulations of the electromagnetic field shielding had been performed using FullWAVE, a package of the commercial software RSoft which solves the Maxwell equations using the finite difference time domain (FDTD) method. Initial test-studies consisted in the investigation of the monitor values in 36 different points, strategically positioned inside the bunker. The distribution of the monitors is done on three parallel planes equally spaced from each other. The FDTD numerical model has calculated the intensity value in all points in arbitrary units, with a quarter of a wavelength accuracy. Thus, we could provide a detailed 3D map distribution of the EM field in the irradiation chamber. The simulations were made on regular computers using scaled configurations setup in order to investigate the field propagation through dispersive media in the vicinity of the focal point inside the interaction chamber assuming the real material properties of the existing building. The geometry of the first approach is depicted in figure 1. The study implies an EM source which has the diameter of 4 μm, vertical polarization and propagates along the x axis. The source is positioned at a distance of 10 μm from the lens which has the focal distance f equal to 10 μm. The frequency is calculated after a complete time response of the monitors is recorded and the Fourier sum is computed. The frequencies are first evaluated in units of μm^{-1} or f/c, where f represents the frequency in Hz and c is the speed of light in vacuum. We analyzed the behavior of the resulted EM field distribution in the focal region using a bulk and a grid dispersive material (SiO_2) as represented in figure 1a and b, with both the thickness and the grid period of 1 μm. For these two cases, we designed quasi-similar experimental setups excepting the absorption element properties.

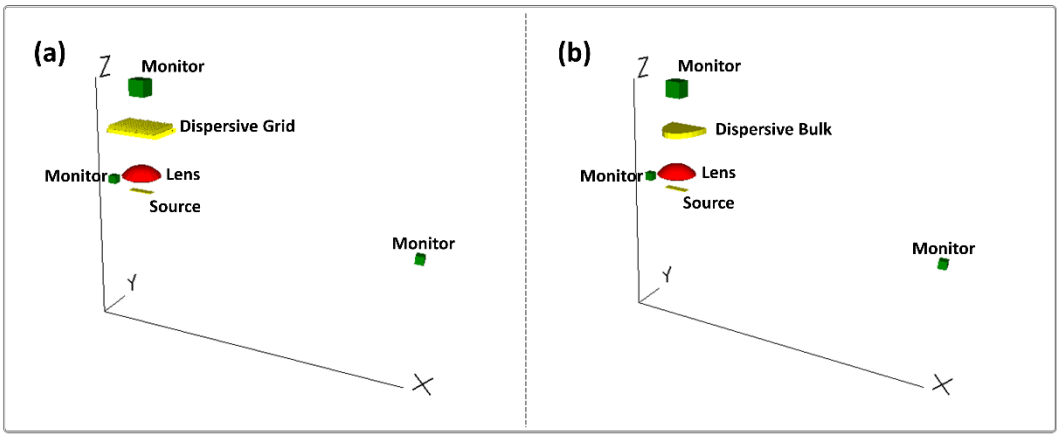

FIG. 1. Sketch of the conceptual setup for electromagnetic field propagation through dispersive media: a) bulk and b) grid material

Figure 2 depicts a comparison between bulk and grid shielding performances for some relevant frequency values in biological environment. As it can be seen, at lower frequencies, the shielding efficiency seems to be slightly greater for the bulk material case. However, at higher frequencies, the difference between the monitor values registered for these two cases is uniformly diminishing. For frequencies values comprises in the range of 600 – 1000 MHz, the EM field shielding presents a similar behavior for both cases investigated.

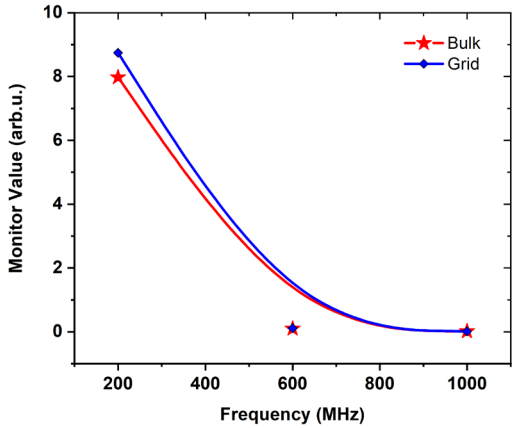

FIG. 2. The frequency evaluation in the vicinity of the focal region for bulk and grid dispersive material

Further, we performed an extended study for frequencies values varying in the range of 100-4000 MHz considering as shielding structures several metallic (copper) cages with micro-structured walls (fig. 3a and b). The 3D design of the conceptual setups has been performed using the above-mentioned numerical model based on FDTD method, in accordance with the initial geometrical purposes. The copper cage wall thickness has been considered to be equal to 1 μm both for foil

and grid pattern cases. The grid parameter *a* has been varied in the range of 0.5 – 4 μm maintaining the grid parameter *b* equal to 1 μm for a more detailed analysis of the electromagnetic field shielding behavior in predefined conditions. In both cases, the source-rear-wall cage distance was of 50 μm, with normal irradiation incidence on the internal target positioned in the center of the cage. The EM wave is focalized on the target using an optical lens with the focal distance of 50 μm. For high focusing accuracy, we generated successive sections along the EM wave propagation axis with a precision of λ/4.

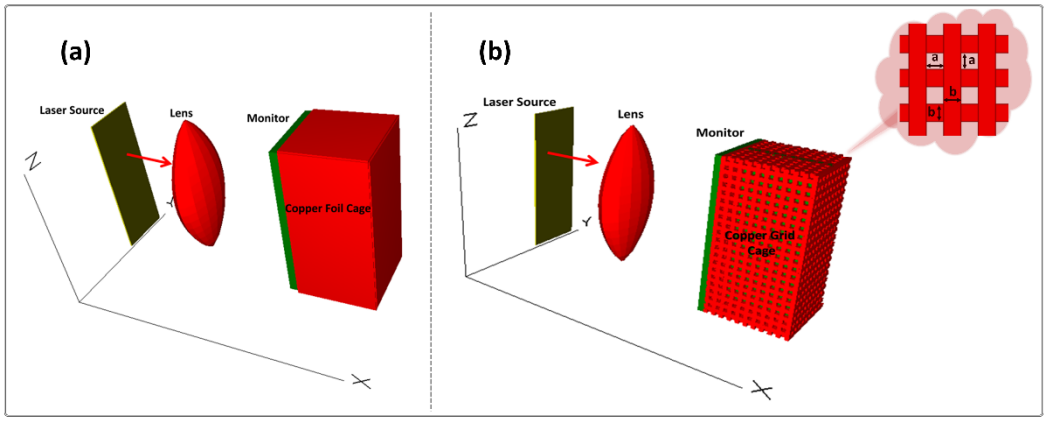

FIG. 3. Design of the conceptual setup for EM field shielding evaluation using metallic structures: a) copper foil wall cage and b) micro-structured wall cage

We analyzed the evolution of the EM field shielding by placing temporal monitors inside the copper cages in similar positions for both cases. One can observe in figure 4 that the monitors registered a similar behavior of the EM field shielding for all five cases analyzed with a minor difference at lower frequencies. For frequencies lower than 300 MHz, the shielding effect present a similar behavior both for *a* parameter values of 1 and 2 μm; for the rest of the frequency range, the shielding effect is slightly greater for the *a* parameter value of 2 μm.

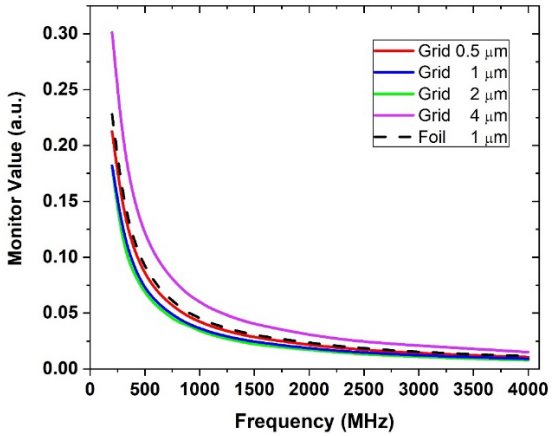

FIG. 4. The electromagnetic field shielding study using different cage wall parameters

As a general remark, the EM field exhibits an accentuated and uniform decrease with the frequency, as in the study depicted in figure 4. This comparison between the grid-walls cases with the foil-wall one, relates that the EM field shielding may be improved in certain conditions.

To deepen the insight of the EM field behavior study in case of using grid-walls cages, we performed an additional analysis considering two different configurations of the cage walls pattern, maintaining the same source parameters and similar setup configuration previously described.

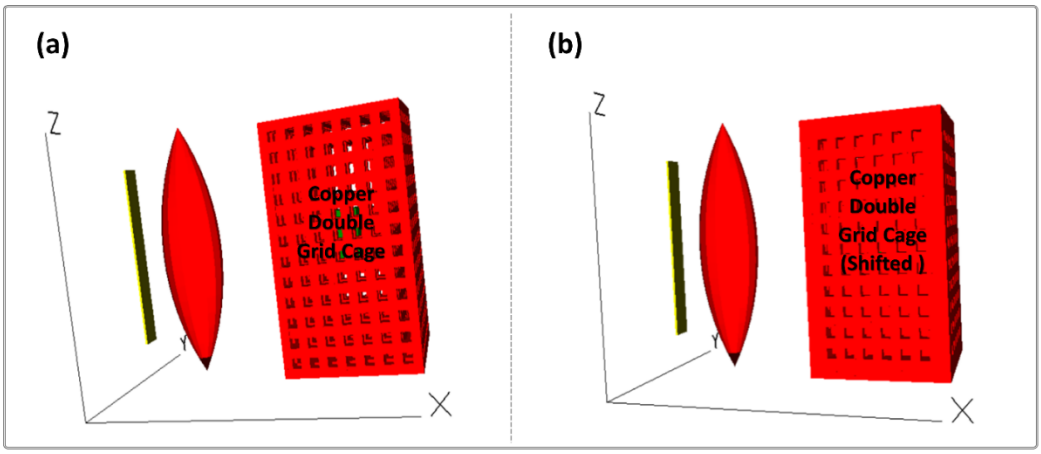

FIG. 5. Sketch of the conceptual setup for EM field shielding evaluation using grid walls structures: a) double-grid walls cage and b) shifted double-grid walls cage

As depicted in figure 5, the cage walls present a parallel (a) and shifted (b) double grid layer having both the grid parameters *a* and *b* equal to 2 μm, corresponding to the ideal case with highest shielding efficiency as evidenced in figure 4. The distance between the layers has been considered to be equal to 2 μm for all numerical computations. By investigating the evolution of the EM field propagation in the both new setup configurations in the presence of the frequency variation in the range of 100-4000 MHz, we could provide the data related to the field shielding, as plotted in figure 6. The numerical simulations show a similar behavior of the EM field shielding for both cases with a slightly greater efficiency in the parallel double grid case denoted by reduced monitor values comparing to the previous approach. In this direction, a complete study regarding the cage walls shift had been performed in order to identify the lowest and the highest field values registered by the temporal monitors. Figure 7 illustrates the evolution of the monitor values in case of shifted cage walls in the range of 0 – 0.25 μm with 0.05 μm step. It can observe a similar behavior of the EM field for symmetric shift values around the reference one which is equal to 0.125 μm and provides the highest field value. Thus, these results reveal that the highest shielding efficiency had been reached by using a double-layer copper cage with no-shifted parallel walls.

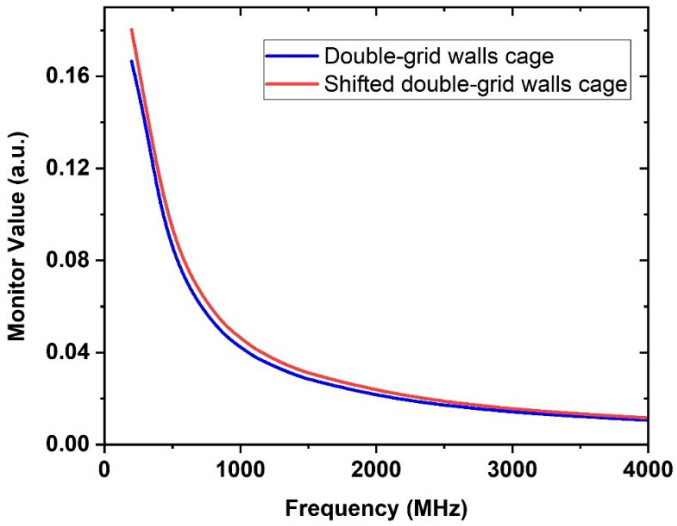

FIG. 6. The electromagnetic field shielding study using two different structures: double mesh cage and shifted double mesh cage

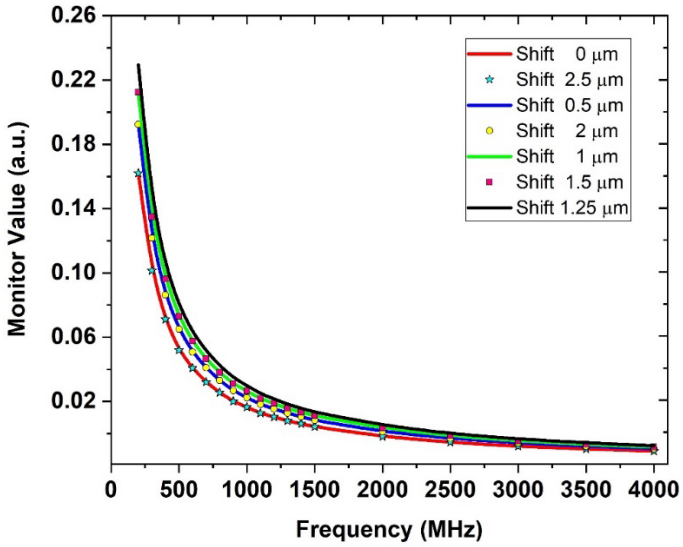

FIG. 7. The evolution of the EM field in in case of shifted cage walls in the range of 0 – 0.25 μm with 0.05 μm step

A complementary study of the electromagnetic field behavior in the presence of *a* parameter variation in the range of 0 – 40 μm has been done for the particular case at 300 MHz frequency, considering a similar setup configuration as depicted in figure 3b. For this study, the copper cage wall thickness has been considered to be equal to 0.5 μm both for foil and grid pattern cases. Measurements of the field intensity inside the cage give a suitable indication of this point.

According to the numerical results presented in figure 8, the shielding effect is significantly sensitive to the grid variation, obtaining a gradual increase of the monitor values around the most efficient *a* parameter value equal to 2 μm. It can be observed that the intensity value registered for *a* parameter value equal to 40 μm is higher with almost 25 percent comparing to the case of *a* parameter value equal to 2 μm and it is almost equal to the intensity value obtained for the case of dispersive metallic foil walls. Moreover, in case of free-space propagation, the beam intensity exhibits an increase with almost 50% related to the ideal *a* parameter value case, proving in this way the efficiency of the structured shielding materials usage in predefined conditions.

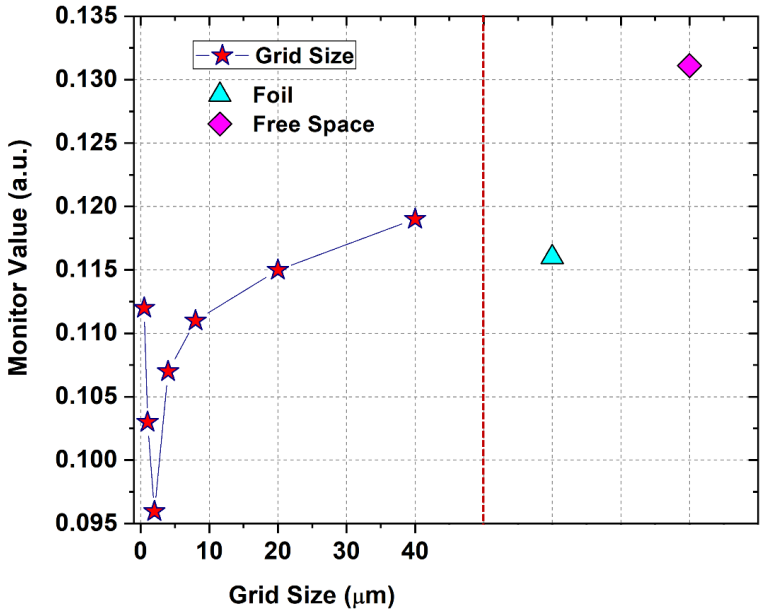

FIG. 8. The electromagnetic field evaluation in the presence of *a* parameter variation at 300 MHz frequency

These results show that the EM field shielding is extremely sensitive on the dispersive materials characteristics and geometrical properties; thus, additional studies regarding the optimization of the material parameters are highly recommended before the experiments. This approach can be used as an alternative model to optimize the setup configurations in the electromagnetic field shielding schemes for experiments in ultra-intense regimes.

4. Conclusions

A numerical analysis concerning the electromagnetic field shielding under high-intensity light irradiation conditions has been elaborated using particular

shielding materials having different profiles in order to measure its efficiency in a wide frequency regime (100-4000 MHz). The FDTD simulations have been performed both for metallic foil and mesh structures. It has been shown that the EM field shielding is extremely sensitive on the dispersive materials properties and the grid structures present a better shielding efficiency comparing to the case of foil structures for specific parameters. Numerical computations at terahertz frequencies are already in progress in order to investigate the efficiency of the configured shielding structures and to monitor the cell behaviour in the vicinity of the petawatt laser irradiation point using the same numerical model based on FDTD method. These studies are important for EM shielding in high energy experiments planned to be performed at ultra-intense laser facilities.

Acknowledgements

This work has been financed by the Romanian Authority for Scientific Research and Innovation NP Nucleu LAPLAS VI 16N/08.02.2019 and by the national project: PN III 5/5.1/ELI-RO, Project 17-ELI/2016 ("BIOSAFE"), under the financial support of Institute for Atomic Physics – IFA**.**

R E F E R E N C E S

[1] *F. Consoli, R. D. Angelis, L. Duvillaret, P. L. Andreoli, M. Cipriani, G. Cristofari, G. G. Di, F. Ingenito, C. Verona*, "Time-resolved absolute measurements by electro-optic effect of giant electromagnetic pulses due to laser-plasma interaction in nanosecond regime," Scientific Reports, 2016; 6:27889

[2] *P. Bradford, N. C. Woolsey, G. G. Scott, G. Liao, H. Liu, Y. Zhang, B. Zhu, C. Armstrong, S. Astbury, C. Brenner, P. Brummitt, F. Consoli, I. East, R. Gray, D. Haddock, P. Huggard, P. J. R. Jones, E. Montgomery, I. Musgrave, P. Oliveira, D. R. Rusby, C. Spindloe, B. Summers, E. Zemaityte, Z. Zhang, Y. Li, P. McKenna D. Neely*, EMP control and characterization on high-power laser systems, High Power Laser Science and Engineering, 2018; 6:e21

[3] *A. Poye, S. Hulin, M. Bailly-Grandvaux, J.-L. Dubois, J. Ribolzi, D. Raffestin, M. Bardon, F. Lubrano-Lavaderci, E. D'Humieres, J. J. Santos, Ph. Nicolaı, V. Tikhonchuk*, Physics of giant electromagnetic pulse generation in short-pulse laser experiments, Physical Review E, 2015; 91: 043106

[4] *M. J. Mead, D. Neely, J. Gauoin, R. Heathcote, P. Patel*, "Electromagnetic pulse generation within a petawatt laser target chamber", Rev. Sci. Instrum., 2004; 75:4225

[5] *M. A. Popovici, F. Negoita, I.O. Mitu, R. Vasilache, D. Buzatu*, Radiological protection calculations of the eli-np 10 pw laser experimental area using fluka code, Romanian Reports in Physics, 2019; 71:208

[6] *T. Liang, J. Bauer, M. Cimeno, A. Ferrari, E. Galtier, E. Granados, H. J. Lee, J. Liu, B. Nagler, A. Prinz, S. Rokni, H. Tran, M. Woods*, Radiation dose measurements for high-intensity laser interactions with solid targets at SLAC, Radiation Protection Dosimetry, 2016; 172:346-355

[7] *M. Numajiri*, Evaluation of the radioactivity of the pre-dominant gamma emitters in components used at high-energy proton accelerator facilities, Radiation Protection Dosimetry, 2007; 123(4): 417–425
[8] *A. Ferrari, E. Amato, D. Margarone, T. Cowan, G. Korn*, Radiation field characterization and shielding studies for the ELI Beamlines facility, Applied Surface Science, 2013; 272:138–144
[9] *G. Florescu, O. G. Duliu*, Shielding activation of petawatt laser facilities in Romania: a FLUKA preliminary evaluation, Radiation Protection Dosimetry, 2015; 168(4):1-4
[10] *O. Dănilă, A. Bărar, M. Vlădescu, D. Mănăilă*-Maximean, An Extended k-Surface Framework for Electromagnetic Fields in Artificial Media, Materials, 2021; 14(24): 7842
[11] *O. Danila,* Polyvinylidene Fluoride-Based Metasurface for High-Quality Active Switching and Spectrum Shaping in the Terahertz G-Band, Polymers, 2021; 13(11): 1860
[12] *M. Mihailescu, I. A. Paun, M. Zamfirescu, C. R. Luculescu, A. M. Acasandrei, M. Dinescu*, Laser-assisted fabrication and non-invasive imaging of 3D cell-seeding constructs for bone tissue engineering, Journal of Materials Science, 2016; 51: 4262–4273
[13] *E. Ionita, A. Marcu, M. Temelie, D. Savu, M. Serbanescu M. Ciubotaru*, Radiofrequency EMF irradiation effects on pre-B lymphocytes undergoing somatic recombination, Sci. Rep., 2021; 11: 12651
[14] *L. Ulrici, Y. Algoet, L. Bruno, M. Magistris*, Radiation protection challenges in the management of radioactive waste from high-energy accelerators, Radiation Protection Dosimetry, 2015; 164 (1-2):112–115
[15] *L. Ulrici, M. Magistris*, Radioactive Waste Management and Decommissioning of Accelerator Facilities, Radiat. Prot. Dosimetry, 2009; 137(1-2):138-48
[16] https://optics.synopsys.com/rsoft/.
[17] *L. Ionel, D. Ursescu*, "Non-collinear spectral coherent combination of ultrashort laser pulses", Opt**.** Express, 2016; 4(7):7046–7054
[18] *L. Ionel, D. Ursescu*, "Spatial extension of the electromagnetic field from tightly focused ultra-short laser pulses", Laser Part. Beams, 2014; 32(1):89-97
[19] *Z. Lin, X. Chen, P. Ding, W. Qiu, J. Pu*, "Modeling the ponderomotive interaction of high-power laser beams with collisional plasma: the FDTD-based approach", Opt. Express, 2017; 25(7):8440-8449
[20] *O. Budriga, L. E. Ionel, D. Tatomirescu, K. A. Tanaka*, Enhancement of laser-focused intensity greater than 10 times through a re-entrant cone in the petawatt regime, Optics Letters, 2020; 45: 3454–7
[21] *O. Budriga, E. d'Humieres, L. Ionel, M. Budriga, M. Carabas*, Modelling the interaction of an ultra-high intensity laser pulse with nano-layered flat-top cone targets for ion acceleration, Plasma Phys. Controlled Fusion, 2019; 61
[22] *L. Ionel,* Spatio-temporal analysis of high-power laser micro-structured targets interaction Phys. Scr., 2020; 95:105501
[23*]* *L. Ionel*, Numerical analysis of non-collinear coherently combined laser beams interaction with micro-structured targets Optics Communications, 2021; 498:127234